Computational Investigation of Structure and Reactivity of Methyl Hydrazinecarbodithioate

Singh, Bhuvanendra
Department of Chemistry, ITM University, Gwalior, INDIA

Singh, Rajeev*+; Singh, Bhoop
Department of Chemistry, Institute of Information Technology and Management, Gwalior, INDIA

Kumar, Dilip
Centre for Research for Chemical Sciences, Post Graduate Department of Chemistry, SMS Govt. College, Gwalior, INDIA

ABSTRACT: *In this study, we theoretically investigated Methyl hydrazinecarbodithioate by quantum chemical calculations for geometry optimization, vibration frequencies, and electronic structure parameters. The geometry optimization by DFT, ab initio MP2 method and the frequency calculation by DFT method was performed at the highest available Pople style 6-311G++(3df,3pd) basis set level. The semi-empirical calculations were performed by the latest PM7 method. The theoretically obtained results were compared with the experimental data. Conformational behavior, frontier molecular orbitals, molecular electrostatic potential, electron localization function, and non-covalent interaction plots were also analyzed. The study explained the geometry, conformational flexibility and relative stability of different conformers.*

KEYWORDS: *DFT; Electron localization function; MP2; Molecular electrostatic surface potential; PM7.*

INTRODUCTION

Methyl hydrazinecarbodithioate (MHC), commonly known as *S*-methyldithiocarbazate (SMDTC) is a methyl ester of Dithiocarbazic acid. Dithiocarbazic acid and its derivatives are known for a long time and they have been compounds of interest among researchers due to their promising use as an active pharmaceutical ingredient for the biological activities shown by them [1]–[9]. In general, the biological activity of a molecule is an outcome of their physical molecular structure and chemical reactivity which depend more specifically on their conformational and tautomeric behavior, hydrogen bonding capability and electronic structure. Peculiarity associated with Dithiocarbazates is the presence of four potential hard and soft nitrogen-sulfur donor atoms and two out of them can chelate with a metal ion subject to steric availability. SMDTC is found to be biologically active [8].

* *To whom correspondence should be addressed.*
+ *E-mail: rajeevs_rathore@rediffmail.com*
1021-9986/2018/2/117-131 15/$/6.05

This compound is especially interesting as it is a single member of this class of compounds found to exist in three conformations [10]. So it is worth to investigate a biologically active molecule having four potential donor atoms with an exceptional capability to existing in different conformational forms. It is considered important to describe its molecular parameters, electronic structure, and reactivity aspect. This study investigates the optimized geometry, vibrational spectra and electronic structure of SMDTC by quantum chemical calculations. For achieving maximum computational accuracy the calculations were performed using the highest available Pople style 6-311G++(3df,3dp) basis set for *ab initio* and DFT methods. The aim of this study is to investigate the structure and reactivity of SMDTC in-depth theoretically to gather computational data for this compound and to compare theoretical predictions with experimental observations. These calculations are valuable as they have been performed at the highest available Pople style basis set level and the data gathered is also valuable for providing insight into the molecular and electronic structure of SMDTC.

COMPUTATIONAL METHODS

The semi-empirical calculations were performed using MOPAC 2012 [11] software. The DFT and MP2 calculations were performed using ORCA computational chemistry package version 3.0.3 [12] in parallel processing mode on Debian 8.0 Linux operating system. Avogadro molecular design and visualizer application version 1.0.3 was used for drawing the molecule [13]. The initial optimization and the lowest energy conformer search was done by molecular mechanics (MM) method using MMFF94 molecular force field [14] and conjugate gradient algorithm at the default 10e-7 convergence set. The initial input geometries of different conformers were generated by rotating MM optimized geometry for appropriate angles about N2-C5 and C5-S8 bonds. These structures were used further as input geometry for geometry optimizations by different quantum chemical methods. Input files were prepared by modifying the files generated with Gabedit Graphical User Interface (GUI) version 2.4.8 [15]. Gabedit was also used for post-quantum chemical calculation result parsing, visualization, and interpretation of the results.

The PM7 semi-empirical geometry optimization calculations in gaseous and solution phase were performed on a WINDOWS based PC system. The DFT and MP2 quantum chemical calculations were performed at 6-311G++(3df,3pd) basis set level [16]–[20]. B3LYP (20 % HF exchange) functional was used for all the DFT calculations. For the calculation of noncovalent interaction, the DFT-D3BJ method was used which includes dispersion correction with Becke-Johnson damping [21,22]. The theoretical assignment of the calculated wavenumbers was done with Gabedit and with aid of the vibrational animation utility of Jmol Java molecular viewer.

RESULTS AND DISCUSSION

Structure and geometry optimization

SMDTC has four possible planar conformers as depicted in Fig. 1. Conformer (II) and (III) are found to exist

in the solid state [23] and the conformers (I), (II) and (III) have evidence of their existence in solutions [10]. *Amore-Bonapasta et al*. presented a nice account of the conformational behavior of SMDTC and derivatives [24]. They inferred a high degree of conformational flexibility for N-N-C-S skeleton performing *ab initio* calculations using minimal basis set.

We investigated further the energetics of the possible conformers by PM7 semi-empirical method, DFT/B3LYP and MP2 methods. The calculated heat of formation (HOF) and final energy are given in Table 1.

Semi-empirical calculations show that conformer (I) is thermodynamically most stable of all conformers. The difference of HOF between conformer (III) and conformer (II) is only 0.5053 kcal/mol which confirms the feasibility of their interconversion as inferred earlier by Amore-Bonapasta and coworkers [24]. Conformer (IV) show high HOF and it is dropped out for further molecular property calculations. The final energy order for rest conformers is (II) > (III) > (I) for MP2 and DFT methods. The dipole moments show the same order. The least energy conformer (I) shows considerably lower dipole moments than dipole moment shown by other conformers. Conformer (II) show the highest value for final energy and dipole moment and it is supposed to get stabilized in solutions. For analyzing the stability of conformers in solutions, we further calculated HOF in different solvents by PM7 method using Conductor-like Screening Model (COSMO) as implemented in

Table 1: Calculated heat of formation and final energy for possible conformers of SMDTC.

Method	Property	(I)	(II)	(III)	(IV)
PM7	HOF	37.28265	38.83503	39.34033	44.27484
	μ	2.193	4.802	3.801	5.995
DFT	Final Energy	-985.58044	-985.57637	-985.57934	-985.56551
	μ	1.559	4.244	2.970	4.890
MP2	Final Energy	-984.35505	-984.34999	-984.35367	-984.33904
	μ	1.828	4.705	3.256	4.494

HOF: kcal/mol; Final Energy: Hartree; μ: Debye

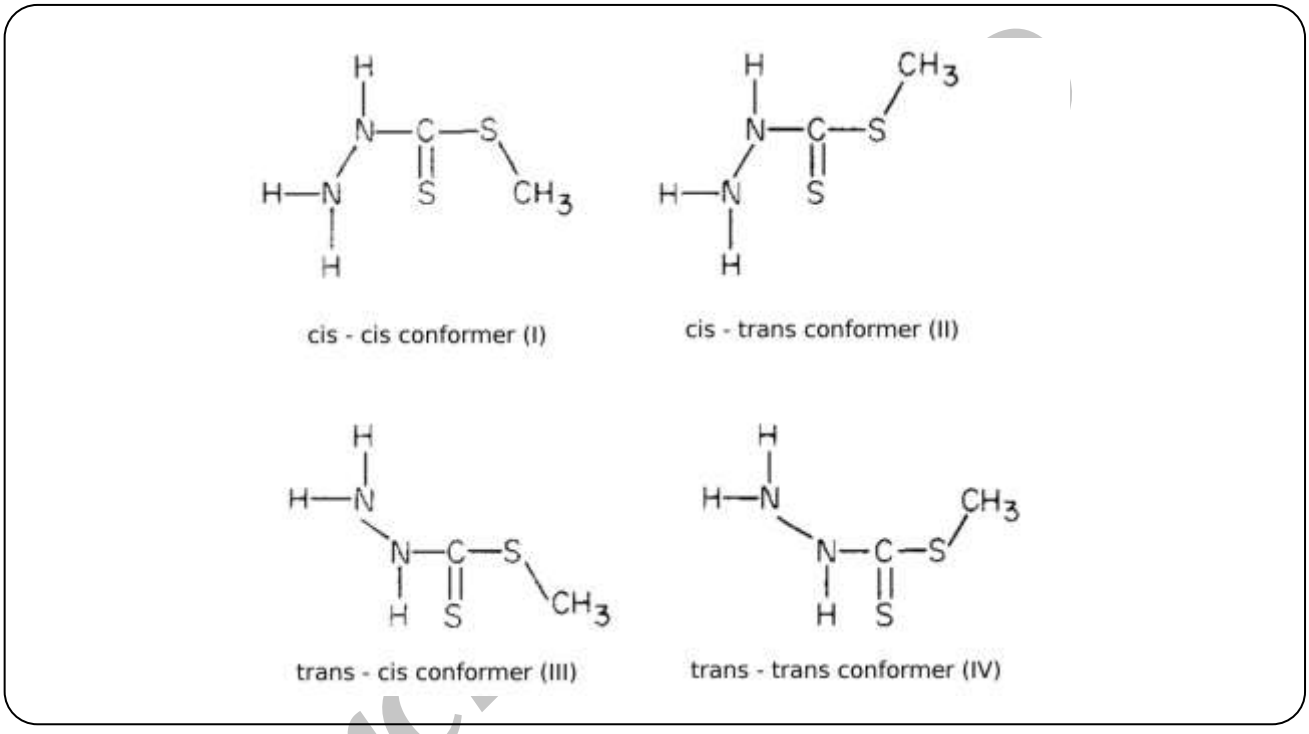

Fig. 1: Possible conformers of SMDTC.

MOPAC2012 (Table 2). Thermodynamic stability of different conformers increases gradually with increasing polarity of the solvents. Conformer (II) is supposed to be most stable in polar media.

DFT calculations produced the best results for geometry optimization in this study. The results obtained by DFT and MP2 calculations for geometry optimization are compared with previously reported X-ray structural data in Table 3. The numbering scheme is given in Fig. 2. Gray, yellow, blue and white color balls show carbon, sulfur, nitrogen and hydrogen atoms respectively. The optimized structures for conformers (I), (II) and (III) are shown in Fig. 3.

In general, the theoretically predicted bond lengths are in good agreement with X-ray crystal structure data. Comparing the theoretical bond angle values with observed bond angle values, we find that most of the optimized bond, angles differ only a little bit from the experimentally observed bond angles. The differences observed between experimentally observed and theoretically calculated values for cis-trans and trans-cis conformers are due to the fact that experimental values of bond angles are measured in the solid state whereas, the theoretical calculations are performed in a gaseous state in absence of any intermolecular solid-state interaction. For conformers (II) and (III) there is a large difference

Table 2: Calculated heat of formation for possible conformers of SMDTC by PM7 method using the COSMO solvent simulation model.

Conf.	Property	DMSO	DMF	CH_3CN	MeOH	Acetone	$CHCl_3$	CCl_4
		47*	38.25*	36.64*	32.6#	21.01*	4.81*	2.24*
(I)	HOF	20.7642	20.9363	21.238 5	21.3285	21.6610	26.0968	30.8862
	μ	5.0073	4.9376	4.9307	4.9268	4.8447	4.0153	3.1534
(II)	HOF	17.4163	17.6674	17.9501	18.1213	18.6623	24.7671	31.0983
	μ	9.2549	9.2378	9.1913	9.1929	9.0278	7.7904	6.4227
(III)	HOF	21.6634	21.6752	21.9131	22.0458	22.4879	27.2425	32.4758
	μ	7.1961	7.1776	7.0839	7.1267	7.0033	6.0594	4.9905
(IV)	HOF	19.7857	20.0408	20.0246	20.2510	21.2511	28.3315	35.5453
	μ	11.333	11.256	11.229	11.212	11.047	9.606	7.986

*HOF: kcal/mol; μ: Debye; * Dielectric constant at 20^0C, # Dielectric constant at 25^0C*

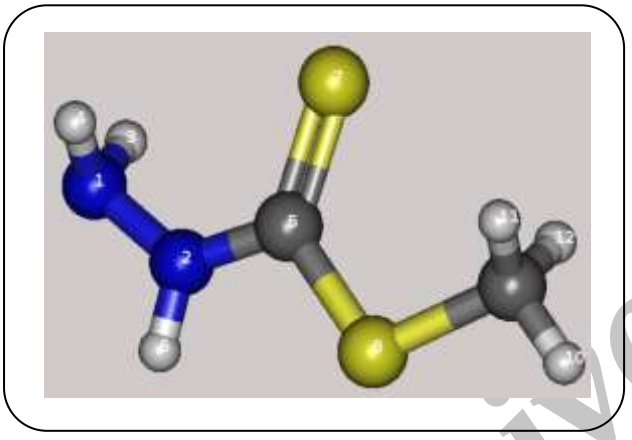

Fig. 2: Atom numbering of SMDTC (cis-cis conformer).

between observed and calculated bond angles values for bonds S7C5S8 and S8C5N2.

In spite of the differences, the calculated geometric parameters show a good approximation to experimental values and they may serve as a basis for calculating other parameters such as vibration frequencies and thermodynamic properties.

The relatively higher theoretical stability of conformer (I) may partly be attributed to intramolecular sulfur centered Non-Covalent Interactions (NCI). For a structurally similar compound, 4-methyl-3-thiosemicarbazide, Francuski, and coworkers inferred that the thioureido =S can be considered as a rather important and potent hydrogen bond acceptor [27]. Allen and coworkers have shown that the thioketonic =S sulfur is more likely to accept more than two hydrogen bonds in comparison to =O acceptor [28]. On this ground, we explored further a possibility for multiple non-covalent intramolecular interactions for thioketonic =S in SMDTC on a theoretical basis. A close look at theoretically calculated values of bond angles reveals that (i) H3N1H4 bond angle value for (I), (II) is lower than that for (III) (ii) H11C9H12 bond angle value for (I) and (III) is lower than that for (II) which suggest a possibility of multiple non-covalent attractive interactions of S7 with H3, H4 and H11, H12 pairs. Noncovalent interaction plots can reveal the nature of weak molecular interactions [29]. Two-dimensional Noncovalent Interaction (NCI) plot of reduced density gradient at sign(λ_2)ρ value - 0.05 to + 0.05 au obtained for SMDTC conformers and their corresponding three-dimensional NCI isosurface plots [29] at iso value 0.6 are shown in Fig. 4. The attractive interactions lay on the left side of zero value and the repulsive interactions lay on the right side of the zero value in 2D plots. 'sign(λ_2)' represents the signature of the second Eigenvalue of Hessian and ρ presents electron density. The low-density, low-reduced gradient troughs having negative values indicate attractive interactions whereas the low-density, low-reduced gradient troughs having positive values indicate steric repulsions. A close look at 2D plots show that noncovalent interactions in conformer, I and conformer III are comparatively stronger than noncovalent interactions in conformer II. Both the attractive and repulsive interactions are present and the overall effect in a conformer will affect its stability. The DFT/6-311G++(3df,3pd) 3D gradient isosurface plots show the existence of intramolecular NCIs in SMDTC conformers. The 3D isosurface is colored on a red-green-blue scale

Table 3: Geometrical parameters calculated by DFT/B3LYP and MP2 methods.

Parameter	(I)		(II)			(III)			% Error			
	Cal.		Cal.		Obs.*	Cal.		Obs.#	(II)		(III)	
	DFT	MP2	DFT	MP2		DFT	MP2		DFT	MP2	DFT	MP2
Bond lengths (Á)												
N1-N2	1.4005	1.3951	1.4040	1.3821	1.415	1.4000	1.3940	1.396	-0.78	-2.33	0.29	-0.14
N2-C5	1.3500	1.3513	1.3468	1.3287	1.315	1.3521	1.3539	1.324	2.42	1.04	2.12	2.26
C5-S7	1.6534	1.6432	1.6563	1.6545	1.679	1.6542	1.6425	1.681	-1.35	-1.46	-1.59	-2.29
C5-S8	1.7772	1.7609	1.7599	1.7525	1.740	1.7728	1.7585	1.745	1.14	0.72	1.59	0.77
S8-C9	1.8052	1.7903	1.8219	1.7973	1.809	1.8057	1.7900	1.803	0.71	-0.65	0.15	-0.72
r^2			0.9890	0.9903		0.9894	0.9881					
Bond Angles (^{0})												
N1N2C5	124.8629	123.9008	124.0724	127.0879	123.6	126.8769	126.0916	121.2	0.38	2.82	4.68	4.04
S8C5N2	110.5094	110.7375	118.0300	113.5363	119.3	112.2016	111.6892	113.6	-1.06	-4.83	-1.23	-1.68
N2C5S7	123.8028	123.4559	124.3008	121.2929	124.5	121.9839	122.5040	120.9	-0.16	-2.58	0.90	1.33
S7C5S8	125.6876	125.8066	117.6691	125.1709	116.2	125.8139	125.8067	125.5	1.26	7.72	0.25	0.24
C5S8C9	102.8744	101.3303	105.9887	103.9153	105.0	102.1564	100.6382	102.6	0.94	-1.03	-0.43	-1.91
r^2			0.9836	0.6260		0.9445	0.9601					
H3N1H4	105.7379	104.8905	105.3537	104.3938		108.8685	108.2105					
H11C9H12	109.9852	109.9610	110.9611	111.1407		109.8213	109.7679					
Dihedrals (^{0})												
N1N2C5S7	-0.171	0.003	-0.038	180.000		179.785	179.961					
N1N2C5S8	179.868	179.979	-179.983	-0.002		0.019	0.028					
N2C5S8C9	-0.612	-179.980	-0.271	179.999		179.962	179.924					
S7C5S8C9	-0.865	-0.005	179.779	-0.002		0.207	-0.006					

Ref. [25], # Ref. [26]

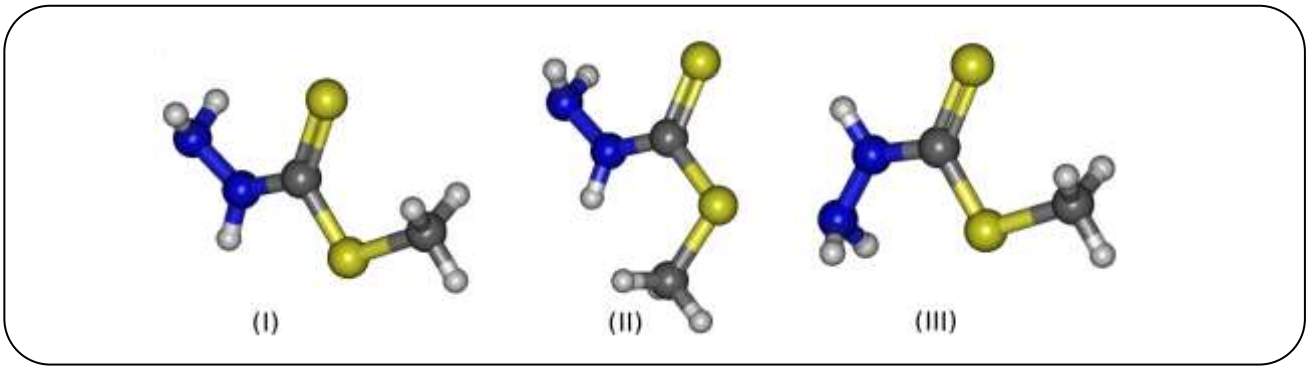

Fig. 3: Different conformers of SMDTC.

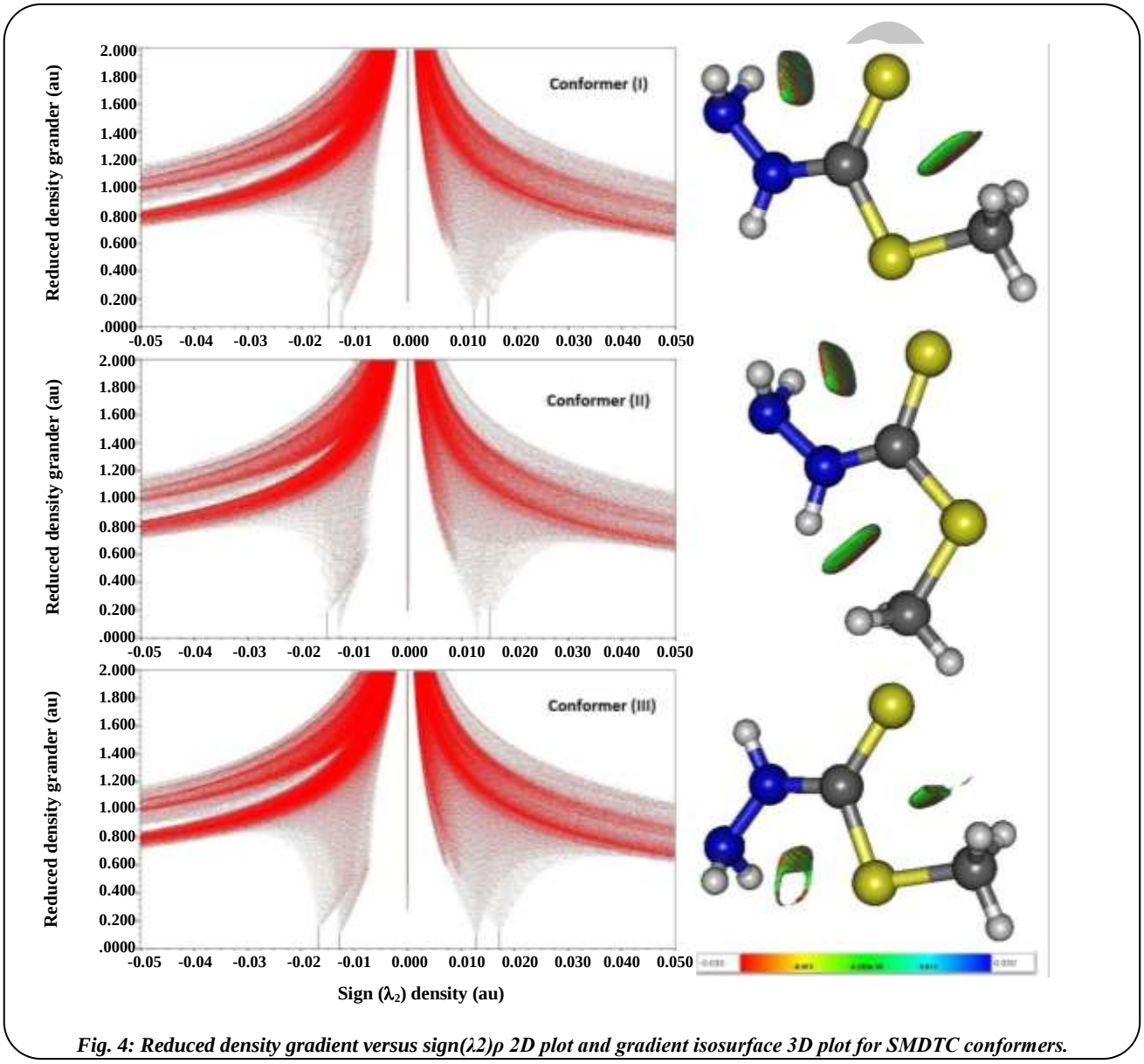

Fig. 4: Reduced density gradient versus sign(λ2)ρ 2D plot and gradient isosurface 3D plot for SMDTC conformers.

according to the values of sign(λ_2)ρ, ranging from -0.03 to 0.03 au. Red indicates strong attractive interactions, green indicates van der Waals interactions and blue indicates strong non-bonded overlap. The 3D plot of NCI for conformer (I) and (III) show comparatively stronger noncovalent interactions in conformer (I). The attractive NCIs are stronger than dispersions but they are not as strong as to be classified under the intramolecular hydrogen bond category.

Vibrational Frequencies

As no scaling factor is available for DFT/6-311G++(3df,3dp) level IR calculations, the unscaled calculated vibrational frequencies are reported as such in Table 4. The difference between calculated and experimental frequencies is due to anharmonic intermolecular interactions, approximation treatment of electronic correlation effects and the limited basis sets. Apart from the numerical difference due to non-scaling, the calculated frequencies show a nice colinearity with experimental frequencies. Only a few discrepancies observed. The δNH assignment of experimental frequencies at 1507 and 1465 is identified as a βN2H6 mode. The observed experimental frequencies 1430 cm^{-1} (δCH_3, rCH_3) and 1421 cm^{-1} (δCH_3) are assigned theoretically as H11C9H12 sci. The experimental δsCH_3 mode at 1290 and 1312 cm^{-1} is predicted theoretically as tH3N1H4. The τNH_2 frequency at 338 cm^{-1} for conformer (II) is theoretically identified as rNH_2 vibration mode. The N-H stretching frequencies for SMDTC are found to be sensitive with respect to structural and electronic changes in –CS-NH- grouping [23]. Manogaran and Sathyanarayana observed NH stretching frequency in 3365-3390 cm^{-1} interval for cis-trans SMDTC and in 3340-3350 cm^{-1} interval for trans-cis SMDTC in the solution phase, i.e. the NH stretching frequency for cis-trans conformer is observed in the higher frequency range in comparison to NH stretching frequency for trans-cis conformer. The theoretical calculations also show the same trend in the gaseous phase. The other conformation sensitive vibrations are N-N stretch, C=N stretch, -NH_2 wagging and twisting and these vibrations show the same trend for the observed frequencies in solid phase and for the calculated frequency values in the gas phase for conformer (II) and (III). The observed values in the solid phase for N-H stretching frequencies for conformer (II) and (III) show an opposite trend in comparison to calculated frequencies for conformer (II) and (III). This opposite trend is easily explicable to N---H and S---H intermolecular hydrogen bonds formed in dimmers of conformer (II) and conformer (III) respectively in the solid crystalline phase [25], [26].

Molecular electrostatic surface potential (MESP)

The MESP is related to the electronic density and it is very useful in determining sites for electrophilic attack and in understanding nucleophilic reactions as well as hydrogen-bonding interactions [30, 31]. 3D MESP plot provides a visual tool to explain electronegativity, partial charges, site of chemical reactivity, structure-activity relationship (SAR), noncovalent bonding, the relative polarity and other interactions of the chemical systems. Mathematically –

$$\text{MESP or } V(r) = \sum_A \frac{Z_A}{|R_A - r|} - \int \frac{\rho(r)}{|r - r|} dr$$

Where Z_A is the charge of nucleus A located at R_A. ρ(r') is electronic density function and r' is an integration variable.

The quantum-chemical calculations can give information on the location of the electron density in the compounds but the local concentration and local depletion of electronic charge density allow us to find out whether an electrophile or a nucleophile can be attracted. MESP was calculated for DFT/6-311G++(3df,3pd) level optimized geometry with MOLDEN package using charge. The color code of 3D MESP plot ranges between −0.1000 a.u. (red) to +0.1000 a.u. (blue) and increases in the order red > yellow > green > sky blue > blue. The red color in Fig. 6 represents a negatively charged area usually associated with the lone pair of electronegative atoms. The negative potential wraps the N1 & N2 atoms. The negative potential also wraps S atoms with a considerably lower value of potential than potential value for N atoms. These negative potential sites *i.e.* the negative region which is localized over N and S atoms are possible sites for the electrophilic attack in SMDTC.

Population Analysis

Population analysis gives an idea of the charge distribution in a molecule. The gross atomic charges provide a means of estimating partial atomic charges and they have an important role in the application of quantum chemical calculations to molecular systems because

Table 4: Selected vibration frequencies for SMDTC experimentally obtained and the calculated vibration frequencies by DFT/6-311G++(3df,3dp) method.

Calculated					Observed*			
(I) Freq.	(II)		(III)		(II)		(III)	
	Freq.	Main Assign.	Freq.	Main Assign.	Freq.	Assign.	Freq.	Assign.
251.67	249.85	δNNC, δNCS	253.19	δNNC, δNCS δCSC	230	δNNC, δNCS	222	δNNC, δNCS δCSC
			276.02	τNH_2	278	πC=S, τCN, τC-S	260	τNH_2, πC=S, τCN
439.51	313.92	δCSC	351.31	δCSC	315	δSCS	350	δCSC, δSCS
463.57		πN2H6 (I)						
566.47	443.47	rNH_2, πN2H6			338	τNH_2, πNH	290	πC=S, τNH_2
684.91	458.50	δNNC, δNCS, νC5S8	505.18	δNNC, δNCS, νC=S	465	νC-S, δNCS	496	δNNC, δNCS, νC=S
	564.68	τCN, τNH_2, πN2H6	550.33	τNH_2, πN2H6	665	τCN, τNH_2, πNH	635	τCN, πNH, τNH_2
			556.29	τCN, πN2H6	665	τCN, τNH_2, πNH	635	τCN, πNH, τNH_2
721.32		νC9S8 (I)	567.31	νC5S8	705	νC=S, wNH_2	582	wNH_2, νC-S
	700.47	δNNC, δNCS, νS8C9	723.14	νC5S7	725	νS-C	727	νS-C, νC-S
932.77	945.01	wCH_3, νC5S8, νN1N2, wNH2	867.98	wNH_2	780	wNH_2	655	wNH_2, νS-C, νC-S
	956.44	tCH_3	981.75	rCH3	945/ 955	rCH_3	949	rCH_3
981.09	971.56	wCH_3, δCH_3	985.48	rCH_3, δCH_3	970	rCH_3, δCH_3	964	rCH_3, δCH_3
993.67	1002.88	νC5S8, νNN, wH3N1H4	1054.32	νC5S7, νNN	1005	νNN, νC-S	1080	νNN, νC=S
1203.59	1201.15	νC5S7, νNN, wH3N1H4	1147.91	δNCS, νNN, νC=S	1120	tNH_2	1047	tNH_2
1346.73	1332.99	δsCH3, νN2C5			1155	δNCS, νNN, νC=S	1170	δNCS, νC=S, νC-S
1347.81	1349.93	tH3N1H4	1318.85	tH3N1H4	1290	δsCH_3	1312	δsCH_3
1369.92	1366.22	νN2C5, δsCH3	1336.47	νN2C5	1373	δNH, νCN, νC=S	1340	νCN, δNH
1451.33	1473.73	δaCH_3	1451.94	δaCH_3	1420	δaCH_3	1412	δaCH_3
1471.66	1480.90	H11C9H12 sci.	1466.80	H11C9H12 sci.	1430	δCH_3, rCH_3	1421	δCH_3
1497.83	1496.27	βN2H6	1481.97	βN2H6, νCN	1507	νCN, δNH	1465	δNH, νCN
1697.76	1699.25	H3N1H4 sci.	1680.48	H3N1H4 sci.	1598	δNH_2	1610	δNH_2
3050.38	3028.14	$vsCH_3$	3052.68	vsCH3	2890	$vsCH_3$	2920	$vsCH_3$
3152.86	3107.78	vaH11C9H12	3140.76	vaCH3	2960	$vaCH_3$	2975	$vaCH_3$
3138.73	3121.64	vaH10C9H12	3156.18	vaH11C9H12	2975	νCH_3	2975	νCH_3
3441.99	3439.12	vsH3N1H4	3458.91	vsH3N1H4	3155	νNH_2	3175	νNH_2
3498.34	3493.65	vaH3N1H4	3536.42	vaH3N1H4	3180	νNH_2	3240	νNH_2
3598.80	3643.06	νN2H6	3602.07	νN2H6	3280	νNH	3305	νNH

**Ref. [23], Freq.: frequency, Assign.: assignment, ν: stretching, δ: deformation, r: rocking, t: twisting, τ: torsion, w: wagging, β: Bending, π: out of plane bending, a: asymmetric, s: symmetric.*

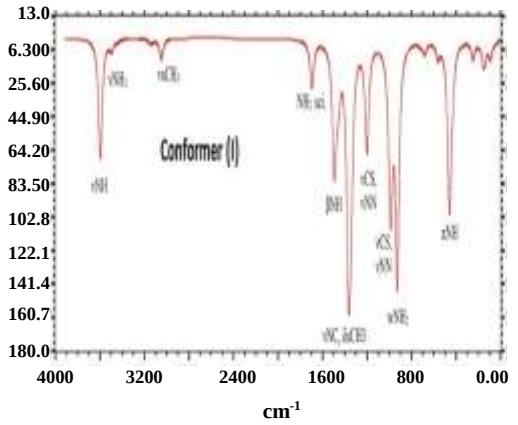

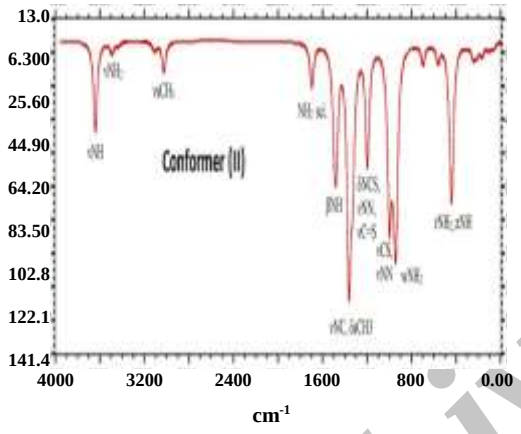

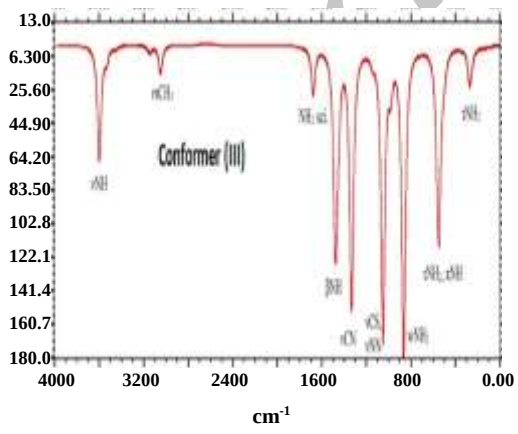

Fig. 5: Theoretical IR spectrums calculated by DFT/6-311G++(3df,3dp) method for SMDTC conformers.

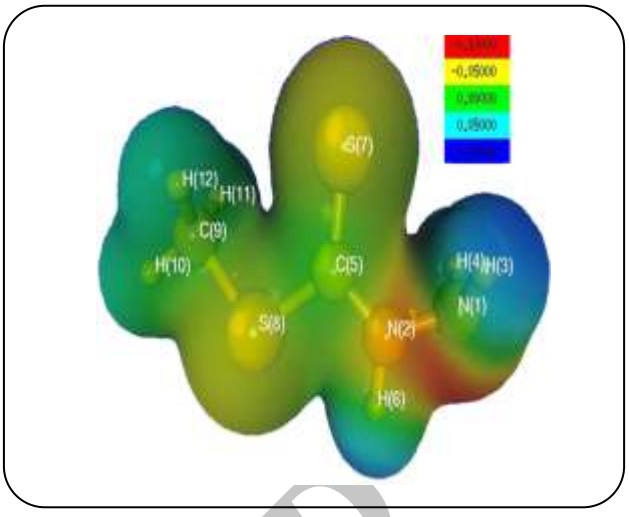

Fig. 6: MESP 3D isosurface plot of SMDTC conformer (I).

atomic charge affects dipole moment, molecular polarizability, electronic structure and a lot of other properties of molecular systems. The natural population analysis of SMDTC produced by an open-source freeware program package JANPA, which produces the same results as the original NBO program [32] is shown as a histogram in Fig. 7. Most negative values predicted stand for C9 atom followed by N1 and N2 atoms, whereas most positive values predicted stand for H6 atom followed by H4 and H3 atoms.

Frontier Molecular Orbital (FMO) analysis

The FMOs of the chemical species are very important in defining its reactivity [33, 34]. The Highest Occupied Molecular Orbital (HOMO) and the Lowest Unoccupied Molecular Orbital (LUMO) are the most important molecular orbitals in a molecule. Higher HOMO energy shows a tendency of a molecule to donate electrons to appropriate acceptor molecule having low energy, empty molecular orbital. Using HOMO and LUMO energy values for a molecule we can compute absolute electronegativity (χ), absolute hardness (η) and softness (s) operationally and approximately [35], [36] as follows-

$$\chi=(I+A)/2 \qquad \eta=(I-A)/2 \qquad s=1/\eta$$

where I and A are ionization potential and electron affinity. Within the limitations of Koopmans' theorem, I and A may be approximated as ($-E_{HOMO}$) and ($-E_{LUMO}$) respectively.

The HOMO and the LUMO energies, the ionization potential (I), the electron affinity (A), the electronegativity (χ),

Table 5: Calculated values of HOMO-LUMO energy, Hardness (η) and related molecular properties for SMDTC conformers by MP2/6-311G++(3df,3dp) method.

Energies/Properties	(I)	(II)	(III)
E_{LUMO+1} (a.u.)	-0.04920	-0.04959	-0.04760
E_{LUMO} (a.u.)	-0.04079	-0.02989	-0.03820
E_{HOMO} (a.u.)	-0.33776	-0.33415	-0.33299
E_{HOMO-1} (a.u.)	-0.34441	-0.33447	-0.33570
$E_{LL\ (HOMO-31)}$ (a.u.)	-91.98381	-91.98906	-91.98795
E_{LUMO} -E_{HOMO} (a.u.)	0.29697	0.30426	0.29479
Energy gap ΔE1 =E_{LUMO+1}-E_{HOMO-1} (a.u.)	0.29521	0.28488	0.28810
Ionization potential (I) = -E_{HOMO} (a.u.)	0.33776	0.33415	0.33299
Electron affinity (A) = -E_{LUMO} (a.u.)	0.04079	0.02989	0.03820
Absolute electronegativity (χ) = (I+A)/2	0.18927	0.18202	0.18559
Absolute hardness(η) = (I-A)/2	0.14845	0.15213	0.14739
Absolute softness (s) = 1/η	6.73469	6.57332	6.78449
Dipole moment (Debye)	1.77741	4.09616	2.76780

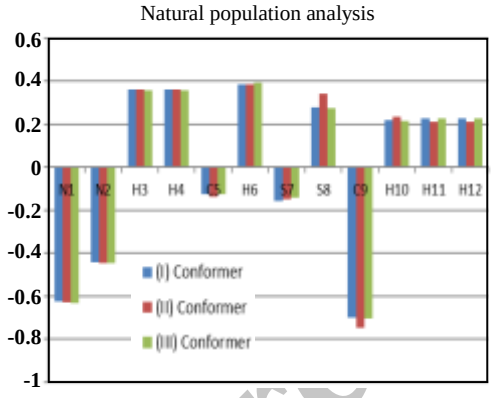

Fig. 7: Histogram of partial charges calculated by DFT/6-311G++(3df,3dp) method for SMDTC conformers.

the chemical hardness and the chemical softness for the title molecule have been calculated by the MP2 method at 6-311G++(3df,3pd) basis set level. The results obtained are given in Table 5. The absolute hardness (η) corresponds to the gap between the HOMO and the LUMO orbital energies. The larger the HOMO-LUMO orbital energy gap the harder the molecule. The hardness has been associated with stability of the chemical systems. An electronic system with a larger HOMO-LUMO gap should be less reactive (less polarizable) than one having a smaller gap [37]. The calculated HOMO-LUMO gap of the molecule by MP2/6-311G++(3df,3pd) comes out as 0.29697, 0.30426 and 0.29479 a.u. for conformers (I), (II) and (III) respectively indicating that the SMDTC is a stable molecule. HOMO-LUMO energy difference order for stable conformers is (I) > (III) > (II), which is the same as the theoretical stability order predicted by PM7 semi-empirical method. The ionization energy (IE) can be expressed through HOMO orbital energy as IE = -E_{HOMO}. The ionization potential values obtained by theoretical study also support the stability of the title molecule. The calculated dipole moment values show that SMDTC is polar in nature.

HOMO-LUMO 3D isosurface plots by MP2/6-311G++(3df,3dp) method for SMDTC conformers are shown in Fig. 8. The blue color illustrates the positive phase of the wave function and the red color illustrates the negative phase of the wave function. The HOMO of SMDTC concentrated over S7 and mainly comprising the nonbonding p orbital of S7 which show electron-rich nucleophilic site in the molecule. The LUMO mainly concentrates over C9, S8 for conformer (I), over C9, S8, N2 for conformer (II) and over C9, S8, N1 for conformer (III).

Electron localization function plot

Becke and *Edgecombe* [38] propounded electron localization function (ELF) as a simple measure of

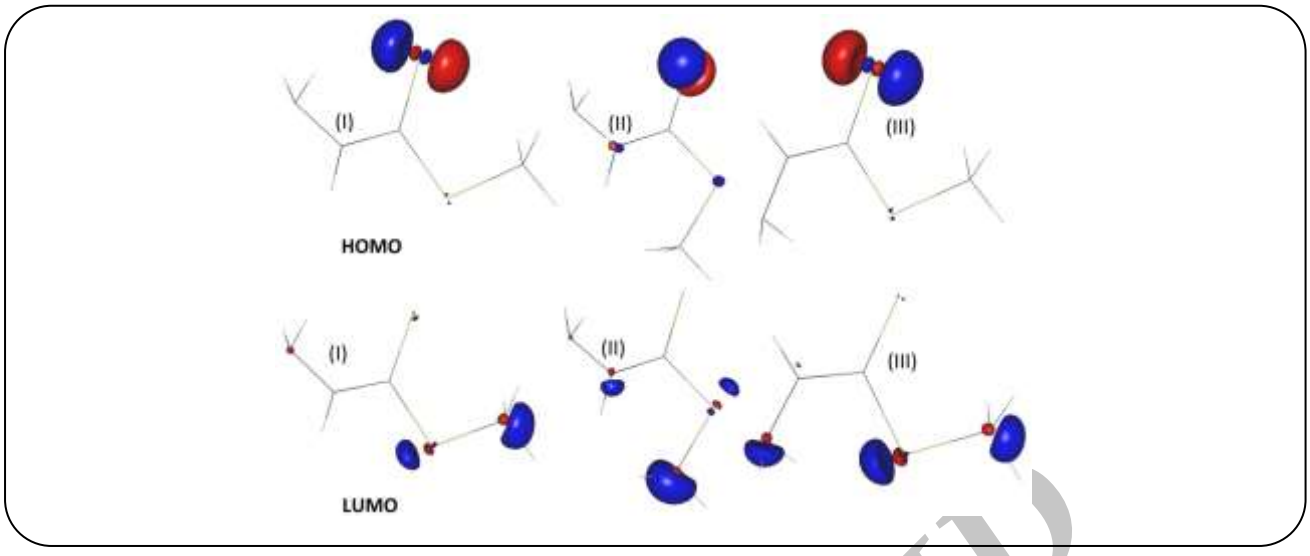

Fig. 8: HOMO-LUMO 3D isosurface plots by MP2/6-311G++(3df,3dp) method for SMDTC conformers.

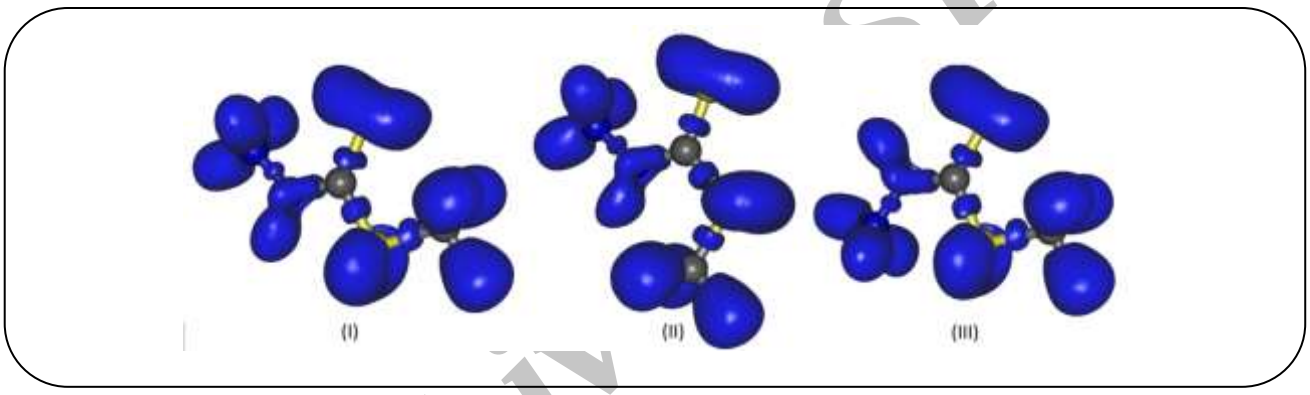

Fig. 9: ELF of SMDTC conformers at level 0.8.

localization of electron in atomic and molecular systems. They defined ELF as follows –

$$ELF(r)=\frac{1}{1+\chi_\sigma^2(r)} \quad 0 \le ELF \le 1, \text{ where } \chi_\sigma^2(r)=\frac{D_\sigma}{D_\sigma^0}$$

where D_σ is the difference of kinetic energy density of the noninteracting system and von Weizsacker kinetic energy density, D_σ^0 is the value of $D_{\sigma the}$ term for homogeneous electron gas. Savin further generalized the ELF approach to a variety of chemical systems [39]. The ELF isosurface plots explain the type of bonding in a chemical species. The ELF 3D isosurfaces [40] for different conformers of SMDTC are shown in Fig. 9. Attractors and basins are the same for all the conformers and they show the same bonding for them. Nonbonding ring attractor domain is visible on S7. The two lone pairs of electrons in the S8 atom are clearly shown in *anti* position. The small ring-shaped circular region between two core regions show typical C–S, N-N single bonds. A single bean shaped V(C, S) disynaptic basin arose for the C5=S7 bond. The nonbonding valence basins of N atoms are visible merged with nearby bonding basins. The V(C, H) disynaptic basins show their typical shape.

CONCLUSIONS

The quantum chemical calculations have been carried out on the molecular geometry, vibration frequencies, HOMO-LUMO energy gap, molecular hardness, ionization energy, dipole moment and total energy. Non-covalent interactions, ELF and MESP plots were analyzed. Frequency calculations found consistent with the observed spectra. The conformational flexibility of SMDTC as inferred by earlier researchers has been

confirmed in this study also. Conformer (I) is found most stable form in the gas phase and conformer (II) is found most stable form in the liquid phase. The non-covalent interaction plots indicate the presence of attractive interactions and steric repulsions in this molecule. The MESP analysis indicates the nitrogen and sulfur atoms as possible sites of electrophilic attack. The ELF isosurface plots show typical localization domains for SMDTC.

Acknowledgments

Rajeev Singh and Bhoop Singh gratefully acknowledge the financial support for this work by the Madhya Pradesh Council of Science and Technology (MPCST), Bhopal by means of Research Grant No. 1076/CST/R&D/2012.

Received: Dec. 20, 2016; Accepted: Jul. 31, 2017

REFERENCES

[1] Cheah, Pike-See, King-Hwa Ling, Karen Anne Crouse R. R., Characterization of the *S*-Benzyldithiocarbazate Effects on Cell Proliferation and Oncogene Expression in Human Breast Cancer Cells, *Med. Biol. Sci.*, **1**(2):1–7 (2007).

[2] Chew K.-B., Tarafder M. T., Crouse K. A., Ali A., Yamin B., Fun H.-K., Synthesis, Characterization and Bio-Activity of Metal Complexes of Bidentate N–S Isomeric Schiff bases derived from *S*-Methyldithiocarbazate (SMDTC) and the X-Ray Structure of the Bis[*S*-methyl-β-*N*-(2-furyl-methylketone)dithiocarbazato]cadmium(II) Complex, *Polyhedron*, **23**(8):1385–1392 (2004).

[3] Crouse K.A., Chew K.-B., Tarafder M.T., Kasbollah A., Ali A., Yamin B., Fun H.-K., Synthesis, Characterization and Bio-Activity of *S*-2-Picolyldithiocarbazate (S2PDTC),Some of its Schiff Bases and Their Ni(II) Complexes and X-Ray Structure of *S*-2-picolyl-β-*N*-(2-acetylpyrrole)Dithiocarbazate, *Polyhedron*, **23**(1):161–168 (2004).

[4] Manan M.A.F.A., Crouse K.A., Tahir M.I.M., Rosli R., How F.N.-F., Watkin D.J., Slawin A.M.Z., Synthesis, Characterization and Cytotoxic Activity of *S*-Benzyldithiocarbazate Schiff Bases Derived from 5-Fluoroisatin, 5-Chloroisatin, 5-Bromoisatin and Their Crystal Structures, *J. Chem. Crystallogr.*, **41**(11):1630–1641 (2011).

[5] Mughrabi F.F., Hashim H., Ameen M., Khaledi H., Ali H.M., Cytoprotective Effect of Benzyl *N'*-(indol-3- ylmethylidene)-hydrazinecarbodithioate Against Ethanol-induced Gastric Mucosal Injury in Rats, *J. Pure Appl. Chem.*, **5**:34–42 (2011).

[6] Mughrabi F.F., Hashim H., Ameen M., Khaledi H., Ali. H.M., Acceleration of Wound Healing Potential of Benzyl *N'*-(Indol-3-Ylmethylidene)-Hydrazinecarbodithioate Derivatives in Experimental Rats, *Res. J. Appl. Sci.*, **5**(2):131–136 (2010).

[7] Pavan F.R., da S Maia P.I., Leite S.R.A., Deflon V.M., Batista A.A., Sato D.N., Franzblau S.G., Leite C.Q.F., Thiosemicarbazones, Semicarbazones, Dithiocarbazates and Hydrazide/hydrazones: Anti-Mycobacterium Tuberculosis Activity and Cytotoxicity, *Eur. J. Med. Chem.*, **45**(5):1898–1905 (2010).

[8] Tarafder M., Kasbollah A., Sarvanana N., Crouse K., Ali A., K T. O., S-methyldithiocarbazate and its Schiff Bases: Evaluation of Bondings and Biological Properties, *J. Biochem. Mol. Biol. Biophys.*, **6**(2):85–91 (2002).

[9] Tarafder M.T.H., Saravanan N., Ali A.M., Kasbollah A., Crouse K.A., Yih K.Y., Some Nitrogen Sulfur Compounds: Bondings and Biological Properties, *Asia Pac. J. Mol. Biol. Biotechnol.*, **9**(1):38–44 (2001).

[10] Gattegno D., Giuliani A.M., NMR Study of Some Derivatives of Dithiocarbazic Acids, *Tetrahedron*, **30**(5):701–704 (1974).

[11] James J. P. Stewart, MOPAC2012.,2012.

[12] Neese F., The ORCA Program System, *Wiley Interdiscip. Rev. Comput. Mol. Sci.*, **2**(1):73–78 (2012).

[13] Hanwell M.D., Curtis D.E., Lonie D.C., Vandermeersch T., Zurek E., Hutchison G.R., Avogadro : an Advanced Semantic Chemical Editor, Visualization, and Analysis Platform, *J. of Cheminf.*, **4**:1–17 (2012).

[14] Halgren T.A., Merck Molecular Force Field. I. Basis, form, Scope, Parameterization, and Performance of MMFF94, *J. Comput. Chem.*, **17**(5–6): 490–519 (1996).

[15] Allouche A.-R., Gabedit - A Graphical User Interface for Computational Chemistry Softwares, *J. Comput. Chem.*, **32**:174–182 (2010).

[16] Dill J. D., Self-Consistent Molecular Orbital Methods. XV. Extended Gaussian-Type Basis Sets for Lithium, Beryllium, and Boron, *J. Chem. Phys.*, **62**(7):2921 (1975).

[17] McLean A. D., Chandler G. S., Contracted Gaussian basis Sets for Molecular Calculations. I. Second Row Atoms, Z= 11-18, *J. Chem. Phys.*, **72**(10): 5639-5648 (1980).

[18] Francl M.M., Pietro W.J., Hehre W.J., Binkley J.S., Gordon M.S., DeFrees D.J., Pople J.A., Self-Consistent Molecular Orbital Methods. XXIII. A Polarization-Type Basis Set for Second-Row Elements, *J. Chem. Phys.*, **77**(7):3654–3665 (1982).

[19] Blaudeau J.-P., McGrath M. P., Curtiss L. A., Radom L., Extension of Gaussian-2 (G2) theory to Molecules Containing Third-Row Atoms K and Ca, *J. Chem. Phys.*, **107**(13):5016–5021 (1997).

[20] Krishnan R., Binkley J. S., Seeger R., Pople J. A., Self-Consistent Molecular Orbital Methods. XX. A Basis Set for Correlated Wave Functions, *J. Chem. Phys.*, **72**(1):650–654 (1980).

[21] Grimme S., Jens A., Ehrlich S., Helge K., A Consistent and Accurate ab Initio Parametrization of Density Functional Dispersion Correction (DFT-D) for the 94 Elements H-Pu, *J. Chem. Phys.*, **132**:154104 (2010).

[22] Grimme S., Ehrlich S., Goerigk L., Effect of the Damping Function in Dispersion Corrected Density Functional Theory, *J. Comput. Chem.*, **32**(7):1456–1465 (2011).

[23] Manogaran S., Sathyanarayana D. N., Conformational Characterization of S-Methyl Dithiocarbazate by Infrared spectra and Vibrational Assignments, *Bull. Chem. Soc. Jpn.*, **55**(8):2628–2632 (Jun. 1982).

[24] Amore-bonapasta A., Battistoni C., Lapiccirella A., Paparazzo E., A Theoretical Study of the Conformational Behaviour of the *S*-Methyl Ester of Dithiocarbazic Acid, *J. Mol. Struct. Theochem.*, **90**(1–2):1–6 (1982).

[25] Lanfredi A. M. M., Tiripicchio A., Camellini M. T., Monaci A., Tarli F., X-Ray and Infrared Structural Studies on the Methyl Ester of Dithiocarbazic Acid and Its N-Substituted Derivatives, *J. Chem. Soc., Dalt. Trans.*, (5):417–422 (1977).

[26] Mattes R., Weber H., Vibrational Spectra and Crystal and Molecular Structure of *trans,cis-S*-Methyl Dithiocarbazate, a Second Conformer, *J. Chem. Soc. Dalt. Trans.*, (3):423 (1980).

[27] Francuski B. M., Novaković S. B., Bogdanović G. A., Electronic Features and Hydrogen Bonding Capacity of the Sulfur Acceptor in Thioureido-Based Compounds. Experimental Charge Density Study of 4-methyl-3-thiosemicarbazide, *Cryst. Eng. Comm.*, **13**(10): 3580 (2011).

[28] Allen F.H., Bird C.M., Rowland R.S., Raithby P.R., Resonance-Induced Hydrogen Bonding at Sulfur Acceptors in $R_1R_2C{=}S$ and $R_1CS_2^-$ Systems, *Acta Crystallogr. Sect. B Struct. Sci.*, **53**(4):680–695 (1997).

[29] Contreras-García J., Johnson E. R., Keinan S., Chaudret R., Piquemal J.-P., Beratan D. N., Yang W., NCIPLOT: a Program for Plotting Non-Covalent Interaction Regions, *J. Chem. Theory Comput.*, **7**(3):625–632 (2011).

[30] Okulik N., Jubert A. H., Theoretical Analysis of the Reactive Sites of Non-Steroidal Anti-Inflammatory Drugs, *Internet Electron. J. Mol. Des*, **4**:17–30 (2005).

[31] Scrocco E., Tomasi J., Electronic Molecular Structure, Reactivity and Intermolecular Forces: An Euristic Interpretation by Means of Electrostatic Molecular Potentials, *Adv. Quantum Chem.*, 11:115-193 (1978).

[32] Nikolaienko T. Y., Bulavin L. A., Hovorun D. M., Chemistry C., Nikolaienko T. Y., Bulavin L. A., Hovorun D. M., Chemistry C., JANPA: An Open Source Cross-platform Implementation of the Natural Population Analysis on the Java platform, *Comput. Theor. Chem.*, **1050**:15–22 (2014).

[33] Fukui K., Yonezawa T., Shingu H., A Molecular Orbital Theory of Reactivity in Aromatic Hydrocarbons, *J. Chem. Phys.*, **20**(4):722–725 (1952).

[34] Mendoza-Huizar L. H., Rios-Reyes C. H., Chemical Reactivity of Atrazine Employing the Fukui Function, *J. Mex. Chem. Soc.*, **55**(3):142–147 (2011).

[15] Allouche A.-R., Gabedit - A Graphical User Interface for Computational Chemistry Softwares, *J. Comput. Chem.*, **32**:174–182 (2010).

[16] Dill J. D., Self-Consistent Molecular Orbital Methods. XV. Extended Gaussian-Type Basis Sets for Lithium, Beryllium, and Boron, *J. Chem. Phys.*, **62**(7):2921 (1975).

[17] McLean A. D., Chandler G. S., Contracted Gaussian basis Sets for Molecular Calculations. I. Second Row Atoms, Z= 11-18, *J. Chem. Phys.*, **72**(10): 5639-5648 (1980).

[18] Francl M.M., Pietro W.J., Hehre W.J., Binkley J.S., Gordon M.S., DeFrees D.J., Pople J.A., Self-Consistent Molecular Orbital Methods. XXIII. A Polarization-Type Basis Set for Second-Row Elements, *J. Chem. Phys.*, **77**(7):3654–3665 (1982).

[19] Blaudeau J.-P., McGrath M. P., Curtiss L. A., Radom L., Extension of Gaussian-2 (G2) theory to Molecules Containing Third-Row Atoms K and Ca, *J. Chem. Phys.*, **107**(13):5016–5021 (1997).

[20] Krishnan R., Binkley J. S., Seeger R., Pople J. A., Self-Consistent Molecular Orbital Methods. XX. A Basis Set for Correlated Wave Functions, *J. Chem. Phys.*, **72**(1):650–654 (1980).

[21] Grimme S., Jens A., Ehrlich S., Helge K., A Consistent and Accurate ab Initio Parametrization of Density Functional Dispersion Correction (DFT-D) for the 94 Elements H-Pu, *J. Chem. Phys.*, **132**:154104 (2010).

[22] Grimme S., Ehrlich S., Goerigk L., Effect of the Damping Function in Dispersion Corrected Density Functional Theory, *J. Comput. Chem.*, **32**(7):1456–1465 (2011).

[23] Manogaran S., Sathyanarayana D. N., Conformational Characterization of S-Methyl Dithiocarbazate by Infrared spectra and Vibrational Assignments, *Bull. Chem. Soc. Jpn.*, **55**(8):2628–2632 (Jun. 1982).

[24] Amore-bonapasta A., Battistoni C., Lapiccirella A., Paparazzo E., A Theoretical Study of the Conformational Behaviour of the *S*-Methyl Ester of Dithiocarbazic Acid, *J. Mol. Struct. Theochem.*, **90**(1–2):1–6 (1982).

[25] Lanfredi A. M. M., Tiripicchio A., Camellini M. T., Monaci A., Tarli F., X-Ray and Infrared Structural Studies on the Methyl Ester of Dithiocarbazic Acid and Its N-Substituted Derivatives, *J. Chem. Soc., Dalt. Trans.*, (5):417–422 (1977).

[26] Mattes R., Weber H., Vibrational Spectra and Crystal and Molecular Structure of *trans,cis-S*-Methyl Dithiocarbazate, a Second Conformer, *J. Chem. Soc. Dalt. Trans.*, (3):423 (1980).

[27] Francuski B. M., Novaković S. B., Bogdanović G. A., Electronic Features and Hydrogen Bonding Capacity of the Sulfur Acceptor in Thioureido-Based Compounds. Experimental Charge Density Study of 4-methyl-3-thiosemicarbazide, *Cryst. Eng. Comm.*, **13**(10): 3580 (2011).

[28] Allen F.H., Bird C.M., Rowland R.S., Raithby P.R., Resonance-Induced Hydrogen Bonding at Sulfur Acceptors in $R_1R_2C{=}S$ and $R_1CS_2^-$ Systems, *Acta Crystallogr. Sect. B Struct. Sci.*, **53**(4):680–695 (1997).

[29] Contreras-García J., Johnson E. R., Keinan S., Chaudret R., Piquemal J.-P., Beratan D. N., Yang W., NCIPLOT: a Program for Plotting Non-Covalent Interaction Regions, *J. Chem. Theory Comput.*, **7**(3):625–632 (2011).

[30] Okulik N., Jubert A. H., Theoretical Analysis of the Reactive Sites of Non-Steroidal Anti-Inflammatory Drugs, *Internet Electron. J. Mol. Des*, **4**:17–30 (2005).

[31] Scrocco E., Tomasi J., Electronic Molecular Structure, Reactivity and Intermolecular Forces: An Euristic Interpretation by Means of Electrostatic Molecular Potentials, *Adv. Quantum Chem.*, 11:115-193 (1978).

[32] Nikolaienko T. Y., Bulavin L. A., Hovorun D. M., Chemistry C., Nikolaienko T. Y., Bulavin L. A., Hovorun D. M., Chemistry C., JANPA: An Open Source Cross-platform Implementation of the Natural Population Analysis on the Java platform, *Comput. Theor. Chem.*, **1050**:15–22 (2014).

[33] Fukui K., Yonezawa T., Shingu H., A Molecular Orbital Theory of Reactivity in Aromatic Hydrocarbons, *J. Chem. Phys.*, **20**(4):722–725 (1952).

[34] Mendoza-Huizar L. H., Rios-Reyes C. H., Chemical Reactivity of Atrazine Employing the Fukui Function, *J. Mex. Chem. Soc.*, **55**(3):142–147 (2011).

[35] Pearson R.G., Absolute Electronegativity and Hardness Correlated with Molecular Orbital Theory, *Proc. Nati. Acad. Sci.*, **83**(November): 8440–8441 (1986).

[36] Pearson R.G., Chemical Hardness and Density Functional Theory, *Journal of Chemical Sciences*, **117**(5):369–377 (2005).

[37]Kurtaran R., Odabaşıoğlu S., Azizoglu A., Kara H., Atakol O., Experimental and Computational Study on [2,6-bis(3,5-dimethyl-N-pyrazolyl)pyridine]-(dithiocyanato)mercury(II), *Polyhedron*, **26**(17): 5069–5074 (2007).

[38] Becke A.D., Edgecombe K.E., A Simple Measure of Electron Localization in Atomic and Molecular Systems, *J. Chem. Phys.*, **92**(9): 5397-5403 (1990).

[39] Savin A., Nesper R., Wengert S., Fässler T. F., ELF: The Electron Localization Function, *Angew. Chemie Int. Ed. English*, **36**(17):1808–1832 (1997).

[40] Savin A., Silvi B., Colonna F., Topological Analysis of the Electron Localization Function Applied to Delocalized Bonds, *Can. J. Chem.*, **74**:1088–1096 (1996).